Nanofilm Allotrope and Phase Transformation of Ultrathin Bi Film on Si(111)7X7

Nanofilm Allotrope and Phase Transformation of Ultrathin Bi Film on Si(111)-7 × 7

T. Nagao,[1,2,*] J. T. Sadowski,[1] M. Saito,[3] S. Yaginuma,[1] Y. Fujikawa,[1] T. Kogure,[4] T. Ohno,[3] Y. Hasegawa,[5]
S. Hasegawa,[6] and T. Sakurai[1]

[1]*Institute for Materials Research, Tohoku University, Sendai 980-8577, Japan*
[2]*Precursory Research for Embryonic Science and Technology (PRESTO), Japan Science and Technology Agency (JST),
Saitama 332-0023, Japan*
[3]*National Institute for Materials Science, Tsukuba 305-0047, Japan*
[4]*Department of Earth & Planetary Science, The University of Tokyo, Tokyo 113-0033, Japan*
[5]*Institute for Solid State Physics, The University of Tokyo, Kashiwa, Chiba, 277-8581, Japan*
[6]*Department of Physics, The University of Tokyo, Tokyo 113-0033, Japan*
(Received 25 August 2003; published 31 August 2004)

Our scanning tunneling microscopy and electron diffraction experiments revealed that a new two-dimensional allotrope of Bi forms on the Si(111)-7 × 7 surface. This pseudocubic {012}-oriented allotrope is stable up to four atomic layers at room temperature. Above this critical thickness, the entire volume of the film starts to transform into a bulk single-crystal (001) phase, as the bulk contribution in the cohesion becomes dominant. Based on *ab initio* calculations, we propose that the new allotrope consists of black phosphorus-like puckered layers stabilized by saturating all the p_z dangling bonds in the film.

When the size and shape of the materials are down-sized to a nanometer scale, they often reveal anomalous atomic structures as well as exotic functional properties that do not exist in bulk. A variety of novel structures discovered in nanoparticles and nanowires have been attracting broad interest [1–4]. Group V elements are known to show rich allotropic transformation because their semimetallic bonding character can be easily shifted to either the metallic or covalent side, for example, by changing the applied pressure [5–8]. In this context, a question arises whether a new allotrope can be realized by tuning the dimensionality or size, such as thickness of the film, instead of tuning the pressure or temperature.

In this Letter, we report on our finding that ultrathin film of Bi really shows such an allotropic transformation as a function of thickness on the scale of several atomic layers. Our electron diffraction and scanning tunneling microscopy (STM) experiments revealed that, over the wetting layer formed initially on the Si(111)-7 × 7 surface, Bi grows with a new {012}-oriented phase whose structure is significantly different from bulk Bi and that it transforms into the bulk-like single-crystal Bi(001) phase above the critical thickness which increases with the substrate temperature. Our *ab initio* theory revealed that the {012} phase with even-number layers is stabilized by forming a puckered-layer structure. The resulting film is very flat, compared to the growth of any known metal films, reflecting the inherent two-dimensional (2D) structure of this {012} phase. To the best of our knowledge, puckered-layer structure was never observed before except for the case of black phosphorus, which is a famous teratoid phase in group V elements.

Bismuth ultrathin films were grown in ultrahigh vacuum (UHV) and characterized *in situ* using STM and reflection high-energy electron diffraction (RHEED). The spot-profile-analyzing low-energy electron diffraction (SPA-LEED) was performed with momentum reso-
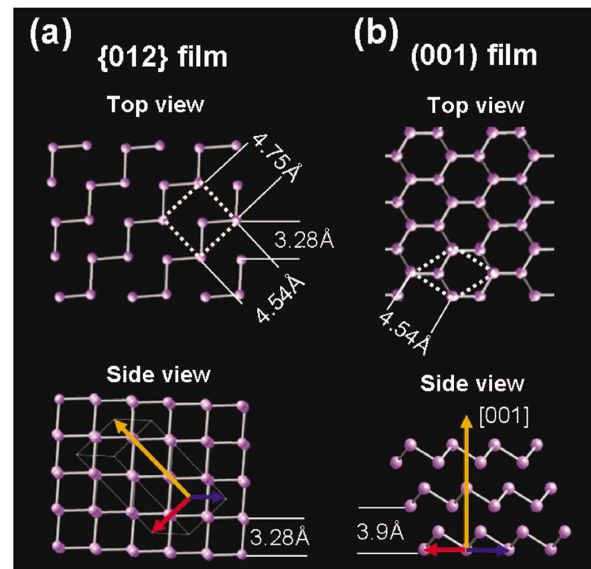

FIG. 1 (color). Schematics of (a) top view and side view of the {012}-oriented phase and (b) top view and side view of the (001)-oriented phase, based on the so-called "distorted A7 structure" of the bulk Bi [5]. The orange arrow is the trigonal **c** axis ([001] axis). Blue and red arrows are [100] and [010] axes (**a** and **b** axes), respectively. The two-dimensional unit cell in the {012} and (001) planes is indicated by each dotted white line.

lution better than 0.006 Å^{-1} in a separate UHV system. All the experiments were performed under a $<1 \times 10^{-10}$ Torr condition. Bi was evaporated from an alumina-coated tungsten basket on a clean Si(111)-7 $\times$ 7 surface (on an n-type $\sim$1 Ω cm wafer) at room temperature (RT). Bi deposition rate was 0.43 ML/min, calibrated by *ex situ* Rutherford backscattering experiments within 6% errors. Here, we define 1 monolayer (ML) as the density of Bi atoms in a pseudocubic Bi{012} plane (9.27×10^{14} atoms/cm^2). For indexing the crystal face of bulk Bi, we adopt here the simplest hexagonal coordinates; $|\mathbf{a}| = |\mathbf{b}| = 4.54$ Å and trigonal axis $|\mathbf{c}| = 11.8$ Å [Fig. 1(b)].

Figures 2(a)–2(d) show the SPA-LEED patterns and Figs. 2(e)–2(h) show the STM images illustrating the evolution of the {012} and (001) phases (stages I to IV) as a function of Bi deposition. Initially a disordered wetting layer forms up to the 1 ML coverage at RT [9,10]. By annealing, it transforms into an ordered β $\sqrt{3} \times \sqrt{3}$-Bi wetting layer. In both cases, we observed the identical Bi allotropic transformation, the main topic discussed in this Letter. Therefore, we exclude the contribution of the initial wetting layer (stage 0) in the discussion and thus the Bi thickness is defined with respect to the wetting layer. In stage I (< 2 ML), while the LEED pattern shows a very weak 7 $\times$ 7 pattern with high background, a so-called Henzler ring is observed [zoomed-in (00) spot as shown in the inset of Fig. 2(a)] [11], indicating the presence of textured islands with

average spacing of 120 Å, consistent with the corresponding STM image in Fig. 2(e). The island height is either 6.6 ± 0.2 or 13.0 ± 0.2 Å, with respect to the disordered wetting layer. Initially, more than 50% of the islands have the lower height, but the higher height islands dominate with increasing thickness.

In stage II (2–4 ML), the LEED pattern shows another texture ring (noted as **R** in Fig. 2(b)]. Ring **R** (1.902 ± 0.002 Å^{-1} in radius) locates slightly outside the silicon (01)-type spots as seen in the inset. This radius precisely matches the distance of the {012}-type plane ($|\mathbf{d}_{012}| = 3.28$ Å in Fig. 1(a)]. Also, the observed STM image with a rectangular surface lattice [4.5 ± 0.2 Å $\times$ 4.9 ± 0.2 Å; inset in Fig. 2(f)] agrees well with the unit cell of the Bi{012} surface [4.54 Å $\times$ 4.75 Å; indicated by dotted lines in Fig. 1(a)]. Island heights measured by STM are consistent with that of the Bi{012} phase. Note an important observation that one of the surface atoms in the unit cell is missing in this STM image, which is discussed later. As shown in Fig. 2(j), the STM profile of the {012} phase shows a height increment of 6.6 ± 0.2 Å, exactly twice the {012} plane distance ($2 \times |\mathbf{d}_{012}|$), which indicates even-number layer stability. Because of this stability, the {012} islands grow laterally flat.

In stage III (4–6 ML), sharp hexagonal spots appear inside ring **R** [Fig. 2(c)]. This hexagonal phase, identified as the Bi(001) phase [see Fig. 1(b)] based on its threefold symmetry and the LEED spot spacing, takes over the {012} ultrathin phase as the film thickness increases. This
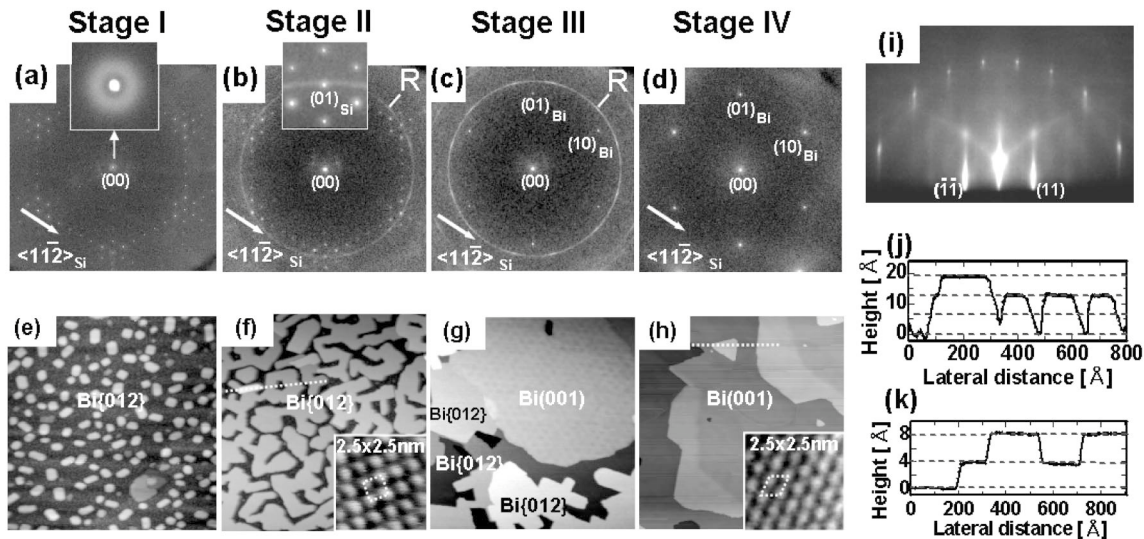

FIG. 2. Evolution of the SPA-LEED pattern (a)–(d), and the STM image (e)–(h) taken at RT as a function of Bi deposition with respect to the wetting layer; stage I (< 2 ML), stage II (2–4 ML), stage III (4–6 ML), and stage IV (> 6 ML). Primary energy of the electron beam in the LEED experiment is 65.0 eV. Insets in (a) and (b) are the magnification around the (00) and the (01) spots, with reciprocal space sizes of 0.26 and 0.32 Å^{-1}, respectively. All the STM images are taken with 1600 Å $\times$ 1600 Å area. Tip bias is (e) 1.0 V, (f) 1.5 V (inset; 1.0 V), (g) 1.0 V, and (h) 1.0 V (inset; 0.1 V). The unit cell of the surface structure is indicated by the white dotted line in the insets in (f) and (h). (i) The RHEED pattern from a 15.2 ML film taken with 15 keV beam energy. (j),(k) STM profiles correspond to the white dotted lines in (f) and (h), respectively.

Bi(001) phase is observed in STM with a very smooth surface [Fig. 2(g)]. In stage IV (> 6 ML), the {012} phase completely disappears and the entire film transforms into the Bi(001) phase and the film morphology becomes very smooth as shown in Fig. 2(h). An inset in Fig. 2(h) shows the atomic image of the Bi(001) phase, which is consistent with the expected unit cell size [4.5 ± 0.2 Å lattice constant in Fig. 1(b)]. The STM height profile of the Bi(001) phase [Fig. 2(k)] shows the step height of 4.0 ± 0.2 Å, which matches that of the Bi(001) bilayer, the structural unit along the trigonal [001] **c** axis [Fig. 1(b)].

The lattice constant of the Bi(001) phase determined by SPA-LEED is 4.480 ± 0.004 Å, compressed by 1.3% from the bulk value in the film parallel direction. This indicates the occurrence of "magic mismatch" between the Bi(001) phase and the Si(111)-7 × 7 surface; that is, the film grows commensurately on the substrate with a relation of $6|\mathbf{a}_{Bi(f)}| = 7|\mathbf{a}_{Si}|$, where $|\mathbf{a}_{Si}| = 3.84$ Å is a unit cell of the Si(111) plane [12]. Therefore, the growth of the Bi(001) phase on the Si(111)-7 × 7 surface has surprisingly perfect azimuthal alignment while it is textured for the lattice-mismatched Bi{012} phase. The observation of Kikuchi lines in RHEED in stage IV manifests the superb crystallinity in the subsurface portion of the film, indicating that the entire volume of the film is highly ordered [Fig. 2(i)].
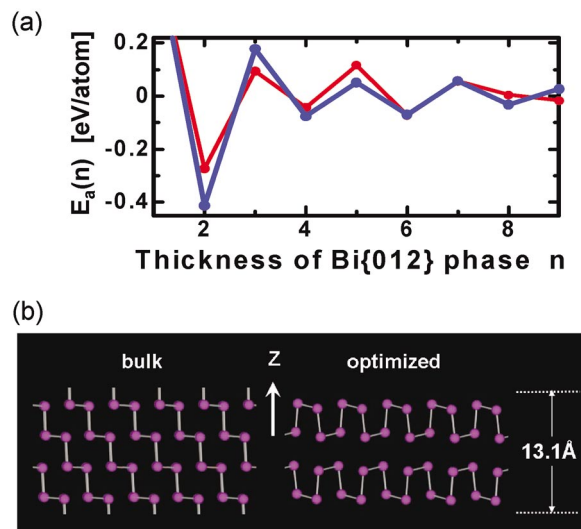

FIG. 3 (color). (a) Calculated layer adsorption energy $E_a(n)$ for the Bi{012} phase with n layers as a function of film thickness for both Bi films with Bi_2H_2 (blue) and BiH_3 (red) wetting layers. Energy is displayed with respect to the bulk cohesive energy. (b). The left-hand side is a side view of a four-layer Bi{012} phase with unrelaxed bulk structure viewed from the [100] direction. The right-hand side is the calculated atomic structure after structural optimization. The intrabilayer structure of this new nanofilm allotrope is analogous to the so-called "puckered-layer structure" of black phosphorus while their stacking sequence is different.

To gain deeper insight into the growth mechanism, we performed *ab initio* total energy calculations based on density-functional theory with the generalized gradient approximation. We employed a norm-conserving pseudopotential with a plane wave basis set, and took 64 **k** points within the 1 × 1 surface Brillouin zone. The calculation was performed for freestanding Bi{012} and Bi(001) slabs as well as for slabs with model wetting layers having different structures, i.e., a hydrogenated Bi monolayer (Bi_2H_2 layer) and BiH_3 molecules with a Bi atom density equivalent to 1 ML, in order to examine the effect of the wetting layer. The results of our *ab initio* calculation are influenced slightly by the modeling of the wetting layer, but this does not contradict the overall observations discussed here.

First, to understand the growth process of the initial {012} phase, layer adsorption energy $E_a(n) = U(n) - U(n-1)$ was calculated, where $U(n)$ is the total energy of the film with n layers [see Fig. 3(a)] [13]. The result indeed supports bilayer growth; films with odd-number layers are unstable and evolve into films with even-number layers. This result explains our STM observations in stages I and II: "high stability" at an even number of layers. This unique film stability can be understood as follows. In an ideal (bulk) {012} phase, 50% of the atoms at the topmost layer have p_z dangling bonds as shown in the left side of Fig. 3(b). In the case of the even-number layer film, all the constituent layers pair up, leading to the complete saturation of the p_z dangling bonds while keeping all the Bi atoms invariably threefold coordinated as in the bulk structure [right side of Fig. 3(b)]. On the contrary, for the case of an odd-number layer film, layer pairing cannot be completed, leaving many dangling bonds. Thus the film is unstable.

The consequence of the pairing relaxation is that it should produce significant buckling at the outermost {012} surface; one of the surface atoms in the unit cell protrudes while the other recedes by as much as 0.5 Å. Indeed, the observed STM image agrees well with this calculated structure, showing only one protrusion in the unit cell as mentioned earlier [inset in Fig. 2(f)]. Also the local density of states at the Fermi level of the paired {012} phase is smaller for both STS and calculation compared with the bulk-like (001) phase, reflecting the reduced metallic nature of this phase due to the bond saturation.

We note that the {012} phase has a striking analogy to the puckered-layer structure of black phosphorus [5,14], except (i) the difference in the stacking sequence of these puckered layers and (ii) strong buckling in each {012} plane. Since such a puckered-layer structure has never been observed under any pressure and temperature conditions among group V elements except phosphorus, this Bi{012} phase is a new allotrope that is realized only at small thickness.
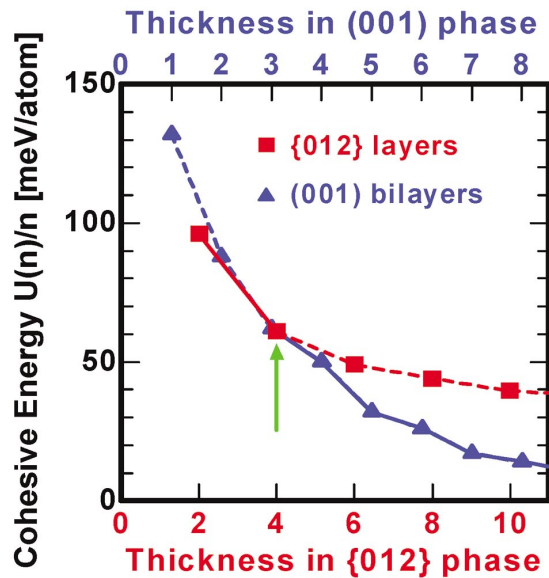
FIG. 4 (color).   Cohesive energy $U(n)/n$ of the {012} and (001) phases calculated as a function of layer thickness n (red and blue curves, respectively). Stable regions are indicated by solid curves and unstable regions in dashed curves. The green arrow indicates the crossover thickness.

Since the amplitude of the energy oscillation in Fig. 3(a) is much larger than the thermal energy ($\sim$ 25 meV), this magic film stability of Bi manifests itself even at *room temperature*. This is in striking contrast to the case of ordinary metals, where 2D growth is realized only at *low temperatures* by electron confinement in the thickness direction [9,10,13,15,16]. We point out that the observed unique 2D growth of Bi is driven by the inherent 2D layered structure of the {012} phase.

In order to quantitatively understand the driving force of the structural transformation from the {012} to the (001) phase, we plotted the cohesive energy $U(n)/n$, or free energy at 0 K, for both phases as a function of film thickness n (Fig. 4). The energy was calculated relative to that of the bulk Bi. $U(n)/n$ of the {012} phase decreases rather slowly as a function of thickness and reaches a plateau at the level of a few tens of meV above the bulk energy, while $U(n)/n$ of the (001) phase rapidly approaches to the bulk energy. Such a difference in the slope of the energy curves yields a crossover of the two phases at 4 ML in the {012} phase, and experimentally, each phase appears in a sequence shown by the solid curves.

Different slopes of the cohesive energy curves can be explained as follows. In the bulk Bi, the Bi atom has three short (stronger) bonds (3.1 Å) and three long (weaker) bonds (3.5 Å). These short and the long bonds correspond to the "intrabilayer" and "interbilayer" bonds of the (001) bilayers, respectively [Fig. 1(b)]. In a hexagonal (001) phase, the surface Bi atoms lose all three long

bonds. On the other hand, in the paired {012} phase, the surface Bi atom loses only one long bond. Therefore, the {012} phase is more stable than the (001) phase at small thickness. As the thickness increases, one can expect that the surface effect becomes less dominant and the cohesive energy swiftly approaches the bulk value. This holds true for the case of the (001) phase which has the bulklike structure. For the case of the paired {012} phase, in contrast, the cohesive energy is smaller than the bulk at a larger thickness because of strain due to buckling. Therefore the stabilization of the puckered-layered {012} phase is possible only at small thickness.

By increasing the substrate temperature from 280 to 310 K, we noticed a slight shift in the crossover thickness. This upward shift in the crossover is reasonable because the {012} phase is likely to have larger entropy than the (001) phase due to its textured nature, and we can expect that free energy $F(n,T) = U(n)/n - TS$ of the {012} phase becomes lower than the relation shown in Fig. 4.

It is noted that the above bond counting scheme is applicable since Bi is semicovalent; the longer interlayer bond still has some bond charge around it and contributes substantially to the cohesive energy. This is in contrast to the ordinary covalent layered crystals, such as graphite, where the contribution from the van der Waals–type interlayer bonds to the cohesion is small.

In conclusion, using STM, SPA-LEED, and first-principles calculations we have successfully documented that a new pseudocubic {012} allotrope phase forms initially and that it transforms into a hexagonal Bi(001) phase, above a critical thickness of 4 ML. The new nanofilm allotrope is stabilized by taking a unique puckered-layer structure.

*Corresponding author.
[1] R. Kubo, J. Phys. Soc. Jpn. **17**, 975 (1962).
[2] S. Ino, J. Phys. Soc. Jpn. **21**, 346 (1966).
[3] H. W. Kroto *et al.*, Nature (London) **318**, 162 (1985).
[4] Y. Kondo and K. Takayanagi, Science **289**, 606 (2000).
[5] H. Iwasaki, and T. Kikegawa, Acta Crystallogr. Sect. B **53**, 353 (1997).
[6] M. I. McMahon *et al.*, Phys. Rev. Lett. **85**, 4896 (2000).
[7] Y. Katayama *et al.*, Nature (London) **403**, 170 (2000); G. Franzese *et al.*, Nature (London) **409**, 692 (2001); T. Morishita, Phys. Rev. Lett. **87**, 105701 (2001); G. Monaco *et al.*, Phys. Rev. Lett. **90**, 255701 (2003).
[8] S. Ostanin *et al.*, Phys. Rev. Lett. **91**, 087002 (2003).
[9] K. Budde *et al.*, Phys. Rev. B **61**, R10 602 (2000).
[10] L. Gavioli *et al.*, Phys. Rev. Lett. **82**, 129 (1999).
[11] K. D. Gronwald and M. Henzler, Surf. Sci. **117**, 180 (1982).
[12] J. Tolle *et al.*, Appl. Phys. Lett. **82**, 2398 (2003).
[13] H. Hong *et al.*, Phys. Rev. Lett. **90**, 076104 (2003).
[14] T. Takahashi *et al.*, Phys. Rev. B **33**, 4324 (1986).
[15] B. J. Hinch *et al.*, Europhys. Lett. **10**, 341 (1989).
[16] I. Matsuda *et al.*, Phys. Rev. B **63**, 125325 (2001).